Australian Journal of Basic and Applied Sciences, 5(12): 300-307, 2011
ISSN 1991-8178

A Novel Weapon Detection Algorithm in X-ray Dual-Energy Images Based on Connected Component Analysis and Shape Features

[1]Hossein Pourghassem, [2]Omid Sharifi-Tehrani and [3]Mansour Nejati

[1,3]Department of Electrical Engineering, Najafabad Branch, Islamic Azad University, Isfahan, Iran.
[2]Young Researchers Club, Majlesi Branch, Islamic Azad University, Majlesi, Iran.

Abstract: Weapon detection is a vital need in dual-energy X-ray luggage inspection systems at security of airport and strategic places. In this paper, a novel weapon detection framework in high-energy images of X-ray dual-energy images based on shape and edge features is proposed. In this framework, image enhancement is carried out by two noise removal and histogram stretching operations. Also, Connected Component Analysis (CCA) is applied to detect weapon candidate regions. An optimum feature set such as Fourier descriptors and invariant moments features are selected by feature forward selection algorithm and used to classify the detected objects into weapon (illicit) and non-weapon (lawful) objects using Probabilistic Neural Network (PNN) classifier. The proposed framework is evaluated on a perfect database consisting of various weapons in different size, type and view and accuracy rate of 96.48% has obtained.

Key words: Weapon detection, dual-energy X-ray, Fourier descriptor feature, probabilistic neural network.

INTRODUCTION

Having tremendous increase of terroristic threat in world, the need for inspection systems in public and strategic places is unavoidable (S. Singh and M. Singh, 2003). For this purpose, dual-energy X-ray luggage inspection systems are playing a basic role in increasing of security at airports, federal buildings. These systems utilize X-rays of two different energies as low-energy and high-energy X-ray. The high-energy X-ray is generated with a high anode voltage around 140 kV, and the low energy X-ray is generated with a low anode voltage around 80 kV (V. Rebuffel and J.M. Dinten, 2007).

In these systems, images are formed based on the energy absorption or transmission by objects (S. Neethirajan *et al.*, 2007). When high-energy X-rays penetrate objects, the energy absorption depends considerably on the material's density. The higher the density is, the higher the energy absorption by the object, and so the darker image formed. For low-energy X-rays, however, the energy absorption depends primarily on the effective atomic number of the material as well as the thickness of the object. However, objects of high density materials such as metal are dark in both low and high-energy X-ray images, but objects of the lighter elements show as darker regions in low-energy images compared to high-energy images. Consequently, the light illicit materials such as explosive, illicit drug can be detected by comparing the low-energy X-ray image with the high-energy X-ray image of the same scene (X.P. He *et al.*, 2008).

Commercial dual-energy X-ray luggage inspection systems fuse a low-energy X-ray image and a high-energy X-ray image into a single image which estimates the atomic number of materials in image of luggage. This estimated atomic number is used to interpret the content of luggage. A limitation on conventional transmission-based X-ray imaging systems is their incapability to differentiate between a thin sheet of a strong absorber and a thick slab of a weak absorber. This problem is usually solved in dual-energy transmission-based X-ray systems by estimating the atomic number of material (S.V. Naydenov *et al.*, 2004).

In this paper, a novel weapon detection framework based on shape features in high-energy images of X-ray dual-energy luggage inspection system is proposed. In this framework, weapon candidate regions are detected based energy absorption of the materials in the X-ray luggage image. Hence, the detected weapon candidate regions are labelled and extracted based on Connected Components Analysis (CCA). Using shape features such as Fourier descriptors and Invariant Moments, Probabilistic Neural Network (PNN) classifier classifies the extracted weapon candidate regions into weapon (illicit) and non-weapon (lawful) objects. The optimum feature vector is formed by feature forward selection algorithm. Using the optimum feature vector, not only the detection performance is improved but also computational complexity is decreased.

Section 2 explains the proposed weapon detection framework. In this section, preprocessing, weapon candidate region detection and feature extraction and selection stages are described. Section 3 introduces

Corresponding Author: Hossein Pourghassem, Department of Electrical Engineering, Najafabad Branch, Islamic Azad University, Isfahan, Iran.
E-mail: h_pourghasem@iaun.ac.ir

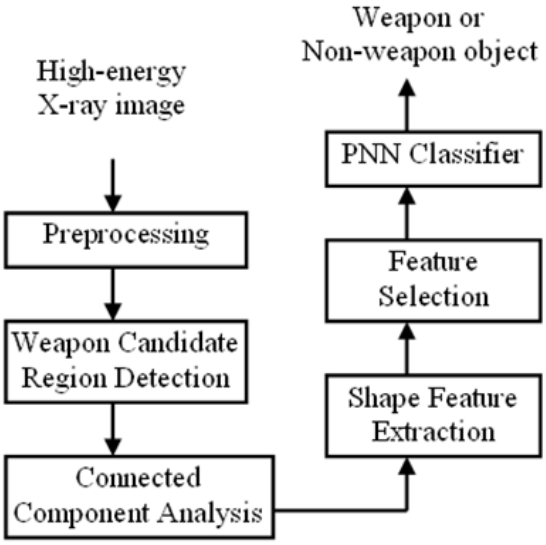

Fig. 1: Block diagram of the proposed weapon detection framework.

PNN classifier. Section 4 shows experimental results on the proposed framework. The concluding remarks and feature research directions are presented in section 5.

The Proposed Weapon Detection Framework:

Fig. 1 shows block diagram of the proposed weapon detection framework. In this framework, weapon candidate regions are extracted from high-energy X-ray image. Using CCA and extracted shape features, PNN classifier classifies the weapon candidate regions to weapon or non-weapon objects. In the following, the details of preprocessing, weapon candidate region detection, CCA, shape features and feature selection algorithm are described.

Pre-Processing:

The high-energy X-ray images usually have considerably noise and low quality. Therefore de-noising and enhancement procedures are two necessary steps in our framework. For this purpose, firstly, a median filter (3×3) is used to cancel salt and pepper noise from the captured images. Secondly, image enhancement carried out using histogram stretching approach which defined as:

$$EF(x,y) = 255 \times \frac{F(x,y) - Min(F(x,y))}{Max(F(x,y)) - Min(F(x,y))} \tag{1}$$

where $EF(x,y)$ and $F(x,y)$ are enhanced and original images, respectively. $Max(.)$ and $Min(.)$ denote maximum and minimum functions, respectively.

Weapon Candidate Region Detection:

When high-energy X-rays penetrate objects, the energy absorption depends on the material's density. The higher the density is, the higher the energy absorption by the object, and so the darker image formed. The illicit weapons are made of metallic materials, so the darker regions in the image are probable metallic objects. To detect the weapon candidate region, pixels of the enhanced image that their values are less than a threshold ($T_{Metallic}$) are selected as metallic object in indexed image.

$$IF(x,y) = \begin{cases} 1 & if\ EF(x,y) < T_{Metallic} \\ 0 & otherwise \end{cases} \tag{2}$$

where $IF(x,y)$ and $EF(x,y)$ are indexed and enhanced images, respectively. $T_{Metallic}$ is selected based on energy level in X-ray image and substance of the desired illicit weapon. In our application, $T_{Metallic}$ is set to 60.

Connected Components Analysis (CCA):

Connected components analysis (CCA) is a well-known technique in image processing that scans an image and labels its pixels into components based on pixel connectivity (i.e., all pixels in a connected component share similar pixel intensity values) and are in some way connected with each other (either four-connected or eight-connected). Once all groups have been determined, each pixel is labeled with a value according to the component to which it was assigned. CCA works on binary or gray-level images and different measures of connectivity are possible. For our application, we apply CCA in binary images searching in eight connectivity. Extracting and labeling of various disjoint and connected components in an image is central to many automated image analysis applications as many helpful measurements and features in binary objects may be extracted, such as area, orientation, moments, perimeter aspect ratio (S.E. Umbaugh, 1998). In this paper, we use area feature such as measure for labeling of the various disjoint and connected components in a high-energy X-ray image. In other word, regions whose areas are more than a predefined threshold are extracted as weapon candidate regions. In this paper, this threshold is set to 200 pixels.

Shape Features:

In this paper, a perfect set of shape and edge features are used to classify the weapon candidate region. Classical shape representation uses a set of invariant moments. We use a set of invariant moments as shape feature of the weapon candidate region. Moreover, a powerful set of edge features that extracted by Fourier transform are used to increase discrimination of the candidate objects. These features are described in the following.

Invariant Moments:

If the object *R* is represented as a binary image, then the central moments of order $p+q$ for the shape of object *R* is defined as:

$$\mu_{p,q} = \sum_{(x,y)\in R} (x-x_c)^p (y-y_c)^q \tag{3}$$

where (x_c, y_c) is the centroid of object. This central moment can be normalized to be scale invariant (L. Yang and F. Algregtsen, 1994):

$$\eta_{p,q} = \frac{\mu_{p,q}}{\mu_{0,0}^{\gamma}}, \gamma = \frac{p+q+2}{2} \tag{4}$$

Based on these moments, a set of invariant moments to translation, rotation, and scale can be derived (S.E. Umbaugh, 1998). In this paper, the first five moments ($\{\phi_1,...,\phi_5\}$) are used (L. Yang and F. Algregtsen, 1994).

Fourier Descriptors:

Fourier descriptors describe the shape of an object with the Fourier transform of its boundary. Consider the contour of a 2D object as a closed sequence of successive boundary pixels (x_s, y_s), where $0 \le s \le N-1$ and *N* is the total number of pixels on the boundary. Then three types of contour representations, i.e., centroid distance, curvature, and complex coordinate function, can be defined (E. Persoon and K. Fu, 1977).

The centroid distance is defined as the distance function between boundary pixels and the centroid (x_c, y_c) of the object:

$$R(s) = \sqrt{(x_s - x_c)^2 + (y_s - y_c)^2} \tag{5}$$

And the curvature $K(s)$ at a point *s* along the contour is defined as the rate of change in tangent direction of the contour, i.e.,

$$K(s) = \frac{d}{ds}\theta(s) \tag{6}$$

Where $\theta(s)$ is the turning function of the contour that is defined as:

$$\theta(s) = \tan^{-1}\left(\frac{y'_s}{x'_s}\right) \tag{7}$$

Where y'_s and x'_s are defined as:

$$y'_s = \frac{dy_s}{ds}, x'_s = \frac{dx_s}{ds} \tag{8}$$

And the complex coordinate is obtained by simply representing the coordinates of the boundary pixels as complex numbers:

$$z(s) = (x_s - x_c) + j(y_s - y_c) \tag{9}$$

To ensure that the resulting shape features of all objects in a database have the same length, the boundary of each object is re-sampled to *M* samples by a uniform sampling function before performing the Fourier transform. The Fourier descriptor of the centroid distance is:

$$f_R = \left[\frac{|F_1|}{|F_0|}, \frac{|F_2|}{|F_0|}, ..., \frac{|F_{M/2}|}{|F_0|}\right] \tag{10}$$

And the Fourier descriptor of the curvature is:

$$f_K = \left[|F_1|, |F_2|, .., |F_{M/2}|\right] \tag{11}$$

And the Fourier descriptor of the complex coordinate is:

$$f_Z = \left[\frac{F_{-(M/2-1)}}{|F_1|}, .., \frac{|F_{-1}|}{|F_1|}, \frac{|F_2|}{|F_1|}, .., \frac{|F_{M/2}|}{|F_1|}\right] \tag{12}$$

Where F_0 and F_1 are DC and the first non-zero frequency components used for normalizing the transform coefficients, respectively. We use the complex coordinate function and the centroid distance representations for our application. In our database, $M = 128$ is set. Therefore, feature vectors of the complex coordinate function and the centroid distance have 126 and 63 elements, respectively.

Feature Selection:

Our goal in feature selection is to find a minimum set of features that is obtained best discrimination between classes. We would like to find the features that most accurately discriminate among the classes and will yield the highest classification accuracy. Since the optimum set of features is unknown, usually two traditional forward selection and backward elimination algorithms are used (A.L. Blum and P. Langley, 1997). The forward selection algorithm starts with an empty set of features and adds one feature at a time until the final feature set is reached. The backward elimination algorithm starts with a feature set containing all features and removes features. The time complexity of the backward elimination algorithm is more than the forward selection algorithm (S.X. Yu, 2005). Therefore, we use the forward selection algorithm as a feature selection algorithm.

Probabilistic Neural Network Classifier:

Basics:

Probabilistic Neural Network is a Bayes-Parzen classifier (T. Masters, 1995). The PNN was first introduced by Specht (D.F. Specht, 1990), who showed how the Bayes-Parzen classifier could be broken up in to a large number of simple processes implemented in a multilayer neural network each of which could be run independently in parallel.

In general, the classification problem can be stated as sampling the p-component multivariate random vector $X = [x_1, x_2, .., x_p]$, where the samples are indexed by k ($k = 1,2,..,K$). The Probability that a sample belongs to the kth population (class) is h_k, the cost associated with misclassifying that sample is c_k, and that the

true probability density function of all population $f_1(x), f_2(x),.., f_k(x),.., f_K(x)$ are know, Bayes theorem classifies an unknown sample into the ith population if:

$$h_i c_i f_i(x) > h_j c_j f_j(x) \tag{13}$$

for all population $j \neq i$. The density function $f_k(x)$ corresponds to the concentration of class k examples around the unknown example. Since the probability density function does usually not know in practice, it is often assumed that they are members of normal distribution. The training set is then used to estimate the parameters of the distribution. However, it is more appropriate to use a nonparametric estimation method such as Parzen windows. In order to classify unknown samples, most common classifiers separate the unknown from each know member of the training set using the Euclidean distance. The unknown member is then classified into the population of its nearest neighbor. The Parzen windows technique goes step further in a way that it takes into account more distant neighbors. Parzen technique estimates a bell-shaped Gaussian function for separating an unknown point from the known training sample point. Such function has a higher value if the distance is close and converges to zero if the distance becomes large. Taking the sum of this function for all known training set members, and classifying the unknown point into the population with the largest sum is the main idea of the probabilistic algorithm. Parzen 's estimated density function is

$$g(x) = \frac{1}{n\sigma^p (2\pi)^{p/2}} \sum_{i=0}^{n-1} e^{\frac{|x-x_i|^2}{2\sigma^2}} \tag{14}$$

Where n is the total number of training examples σ is scaling parameter that controls the width of the area of influence of the distance.

Although the value of the σ is an important smoothing in the probabilistic network since it affects the estimation error; there is no mathematical way of determining it. A too small value of σ gives the same effect as the nearest neighbor technique and a too large σ does not give clear separation of classes and classification can not be made.

Network Operation:

Consider the simple network architecture shown in Fig. 2 with four input nodes (p=4) in the input layer, two population classes (class 1 and class 2), five training examples belonging to class 1 (n_1=5), and three examples in class 2 (n_2=3). The pattern layer is designed to contain one neuron (node) for each training case available and the neurons are split into the two classes. The summation layer contains one neuron for each class. The output layer contains one neuron that operates trivial threshold discrimination; it simply retains the maximum of the two summation neurons. The PNN executes a training case by first presenting it to all pattern layer neurons. Each neuron in the pattern layer computes a distance measure between the presented input vector and the training example represented by that pattern neuron. The PNN then subjects this distance measure to the Parzen window and yield the activation of each neuron in the pattern layer. Subsequently, the activation form each class is fed to the corresponding summation layer neuron, which adds all the results in a particular class together. The activation of each summation neuron is executed by applying the remaining part of the Parzen's estimator equation to obtain the estimated probability density function value of population of a particular class. If the misclassification cost and prior probabilities are equal between the two classes, and the classes are mutually exclusive (i.e., no case can be classified into more than one class) and exhaustive (i.e., the training set covers all classes fairly), the activation of the summation neurons will be equal to the probability of each class. The results from the two summation neurons are then compared and the largest is fed forward to the output neuron to yield the computed class and the probability that this example will belong to that class.

The most important parameter that needs to be determined to obtain an optimal PNN is the smoothing parameter of the random variables. A straightforward procedure involves selecting an arbitrary value of σ 's, training the network, and testing it on a test set of examples. This procedure is repeated for other σ 's and the set of σ 's that produces the least misclassification rate is chosen.

Experimental Results:

Database:

The X-ray image test dataset have captured by a commercial luggage scanner. The perfect dataset of weapons in the various size, type and view has obtained to evaluate the proposed framework. The weapon test dataset is consisting of 200 image samples. Fig. 3 shows the weapon image samples.

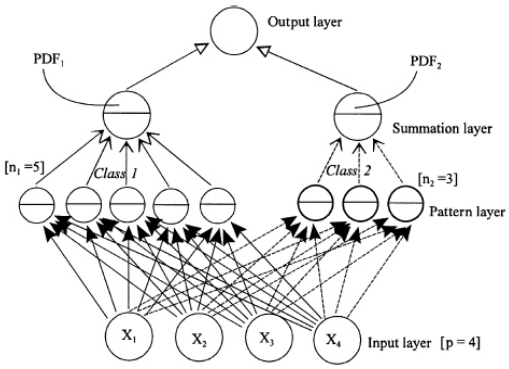

Fig. 2: A simple Probabilistic neural network with four input variables, two classes, and eight training examples.

Fig. 3: Weapon image samples.

Fig. 4: A luggage X-ray image sample.

Weapon Candidate Object Extraction:

Fig. 4 shows a luggage X-ray image which consisting of a gun, a knife, an umbrella and etc. After applying of the preprocessing, weapon candidate detection and CCA stages, the weapon candidate objects are extracted from luggage image. The extracted weapon candidate objects are shown in Fig. 5. The invariant moments and Fourier descriptors features are extracted from the detected weapon candidate binary object and re-sample boundary pixels of the detected weapon candidate objects, respectively. The binary image and successive boundary pixels of a gun and re-sample boundry pixels (M=128) by a uniform function are shown in Fig. 6.

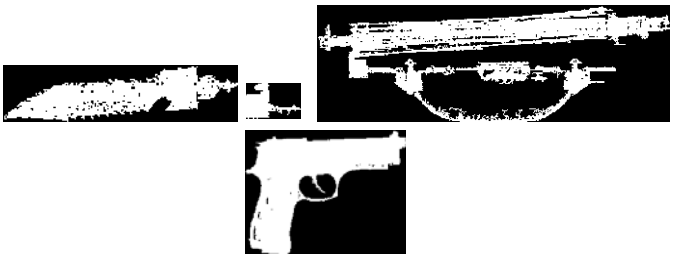

Fig. 5: The extracted weapon candidate objects from image shown in Fig. 4.

(a) (b) (c)

Fig. 6: (a). The binary object, (b). Successive boundary pixels and (c) re-sample boundry pixels of a gun.

Table 1: Classification results with different feature vector and smoothing parameter in PNN classifier.

Feature space(and their weights in feature vector)	Feature length	Smoothing parameter in PNN	Accuracy %
I	5	0.22	43
FZ	126	0.18	82.4
FR	63	0.19	77.6
I (1), FZ (1)	131	0.21	87.24
I (1), FR (1)	68	0.22	78.1
FZ (1), FR (1)	189	0.23	87.73
FZ (1), FR (1), I (1)	194	0.21	91.25
FZ (1.2), FR (1), I (1)	194	0.2	93.36
FZ (1.2), FR (1), I (0.8)	194	0.19	94.32
FZ (1.5), FR (1), I (0.8)	194	0.2	96.48

Feature Selection and PNN Classifier:

Image representations were generated in 7 different feature spaces (Table 1) using the following features: invariant moments (I), Fourier descriptor-complex representation (FZ), Fourier descriptor-centroid representation (FR). PNN classifier was classifeid weapon candidate objects with different feature vectors and smoothing parameters. The optimum smoothing parameter is determined by trial and error approach.

FZ feature obtains higher classification accuracy than FR and I features. So, the weight of FZ is considered higher than weight of others features. Results indicate that the (FZ, FR, I) feature space provides higher classification accuracy than the other options investigated. Accuracy rate 96.48% is obtained with this feature space and (1.5,1,0.8) for its weight.

Conclusions:

Weapon detection is a vital need in dual-energy X-ray luggage inspection systems at security of airport and strategic places. We presented a novel weapon detection framework in high-energy images of X-ray dual-energy based on shape features. In this framework, the quality of input images was improved using two noise removal and histogram stretching operations. Also, the detected weapon candidate regions by CCA was classified based on a perfect set of shape feature such as Fourier descriptors and Invariant moments features and PNN classifier into weapon (illicit) and non-weapon (lawful) objects. The proposed framework was evaluated on a perfect database of gun and real images of luggage. Ultimately, accuracy rate of 96.48% had obtained.

REFERENCE

Blum, A.L. and P. Langley, 1997. “Selection of relevant features and examples in machine learning”, Artificial Intelligence, 97: 245-271.

He, X.P., P. Han, X. G. Lu and R.B. Wu, 2008. “A New Enhancement Technique of X-Ray Carry-on Luggage Images Based on DWT and Fuzzy Theory”, International Conference on Computer Science and Information Technology, pp: 855-858.

Masters, T., 1995. Advanced *algorithms for Neural Networks*, New York, John Wiley and Sons.

Naydenov, S.V., V.D. Ryzhikov and C.F. Smith, 2004. “Direct reconstruction of the effective atomic number of materials by the method of multi-energy radiography”, Nuclear Instruments and Methods in Physics Research, 215: 552-560.

Neethirajan, S., D.S. Jayas, C. Karunakaran, 2007. “Dual energy X-ray image analysis for classifying vitreousness in durum wheat”, Postharvest Biology and Technology, 45: 381-384.

Persoon, E. and K. Fu, 1977. “Shape discrimination using Fourier descriptors”, IEEE Trans. Sys. Man and Cyber., 7: 170-179.

Rebuffel, V. and J.M. Dinten, 2007. “Dual-energy X-ray imaging: benefits and limits”, Insight, 49(10): 589-594.

Singh, S. and M. Singh, 2003. “Review- Explosives detection systems (EDS) for aviation security”, Signal Processing, 83: 31-55.

Specht, D.F., 1990. “Probabilistic neural networks,” *Neural Networks*, 3: 109-118.

Umbaugh, S.E., 1998. *Computer Vision and Image Processing*. Englewood. Cliffs, NJ: Prentice-Hall, pp: 133-138.

Yang, L. and F. Algregtsen, 1994. “Fast computation of invariant geometric moments: A new method giving correct results”, Proc of IEEE ICIP, pp: 201-204.

Yu, S.X., 2005. “Feature Selection and Classifier Ensembles: A Study on Hyperspectral Remote Sensing Data”, PhD Thesis, University of Antwerp.